

PETRA IV ALIGNMENT OVERVIEW

J. Barker*, Deutsches Elektronen-Synchrotron DESY, Hamburg, Germany

Abstract

PETRA IV requires stringent alignment accuracies for close to 300 girders and over 3000 magnets, despite pervasive space constraints. This paper summarizes the alignment progress of the project's current prototype (pre-project) phase, as well as future plans. Under development are two novel multipole magnet referencing concepts photogrammetric and laser tracker measurements. Each concept utilizing laser optical micrometers on a vertical rotary stage axially traversed by a vibrating wire. Also Custom stable floor-mounted instrument pillars are under prototype-phase development. These will be applied to multiple alignment and magnet fiducialization work stations for PETRA IV.

INTRODUCTION

This paper represents the progress during the TDR phase of PETRA IV. It summarizes the testing done in this period and the preparations for the pre-project phase which the project is currently entering. The main goal of the pre-project phase is to finalize prototypes, methods and finishing the proofs of concepts (PoC) for the chosen procedures.

The physics grounds for the stringent accuracies, which are driving enhancements beyond standard procedures, is detailed in [1]. There are currently two approaches under investigation: a laser tracker and a photogrammetry approach. Each has its advantages and downsides, especially regarding the automation requirements. I introduce the advances of the proofs of concept for magnet referencing.

The rapid construction schedule of PETRA IV and ongoing difficulty finding qualified personnel for high accuracy geodetic and metrology work, leads us to anticipate a personnel shortage for the Alignment of PETRA IV. Consequently, we plan to automate high-volume task such as magnet referencing (fiducialization).

Then, in the "Instrument Pillar Design" section, I discuss the design of stable instrument pillars. Currently, after testing two different types, clearer requirements can be set and the design can start.

The last section describes small useful scripts which were developed during the TDR phase. Those scripts are tools for data analysis, visualization, etc.

I wish you a pleasant read.

MAGNET REFERENCING DEVELOPMENT

The very stringent alignment accuracies for the PETRA IV resistive magnets necessitate new referencing strategies and methods. The accuracy, as of now, are defined as the maximum size of the semi-major axis of the

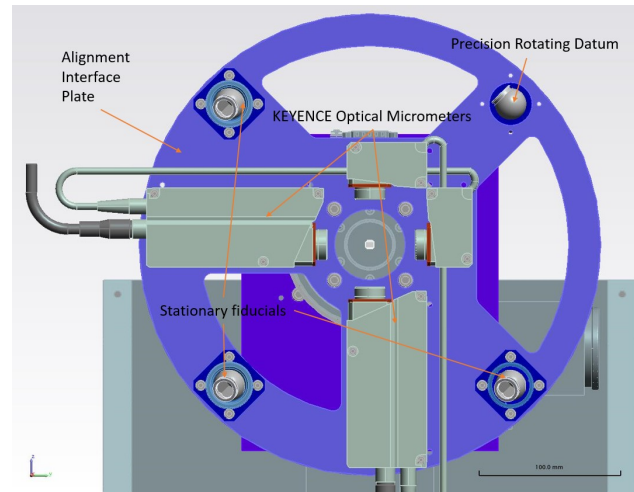


Figure 1: The rotational apparatus for the laser tracker approach. The Alignment Interface Plate rotates on the rotational stage, and holds SMRs and KOMs. [Daniel Thoden]

error ellipsoid at $p=0.68$. The required magnet to magnet accuracy is $30\ \mu\text{m}$ and girder to girder is $100\ \mu\text{m}$.

The Magnet Testing work package is developing a new stretched wire magnet measurement bench, shown in Figure 2. The magnetic axis of the magnet under test is determined by locating where the current induced in the vibrating wire is minimized. The measurement bench has two towers (outer structures), each equipped with two perpendicular linear stages which together carry the wire holder and position the wire. The bench also has two stands (inner structures), each with a rotational stage axially traversed by the stretched wire. The rotational stage holds and rotates the alignment interface plate (AIP). Onto each AIP, two perpendicular Keyence laser optical micrometers (KOMs) are mounted that will measure the position of the wire as the stage rotates around it, see Figure 1 for detail. The KOM will measure in the direction of one coordinate axis of a roughly perpendicular coordinate system (KCS).

The decision has not yet been made as whether to placing a set of linear stages between stands and rotational stage. Currently two approaches are being developed and tested: the laser tracker and the photogrammetry approaches. There are two main goals of the development - automatization of the whole process and pushing the overall accuracy of fiducialization below $15\ \mu\text{m}$. That includes the magnetic axis determination, measurements of the position of the wire and referencing it to the fiducials on the magnet. Experience and predictions indicate there will not be enough metrology technicians to reference the 2659 resistive magnets that will make up PETRA IV. The idea is to have an automated system instructing the non-expert alignment operators of actions,

* jana.barker@desy.de

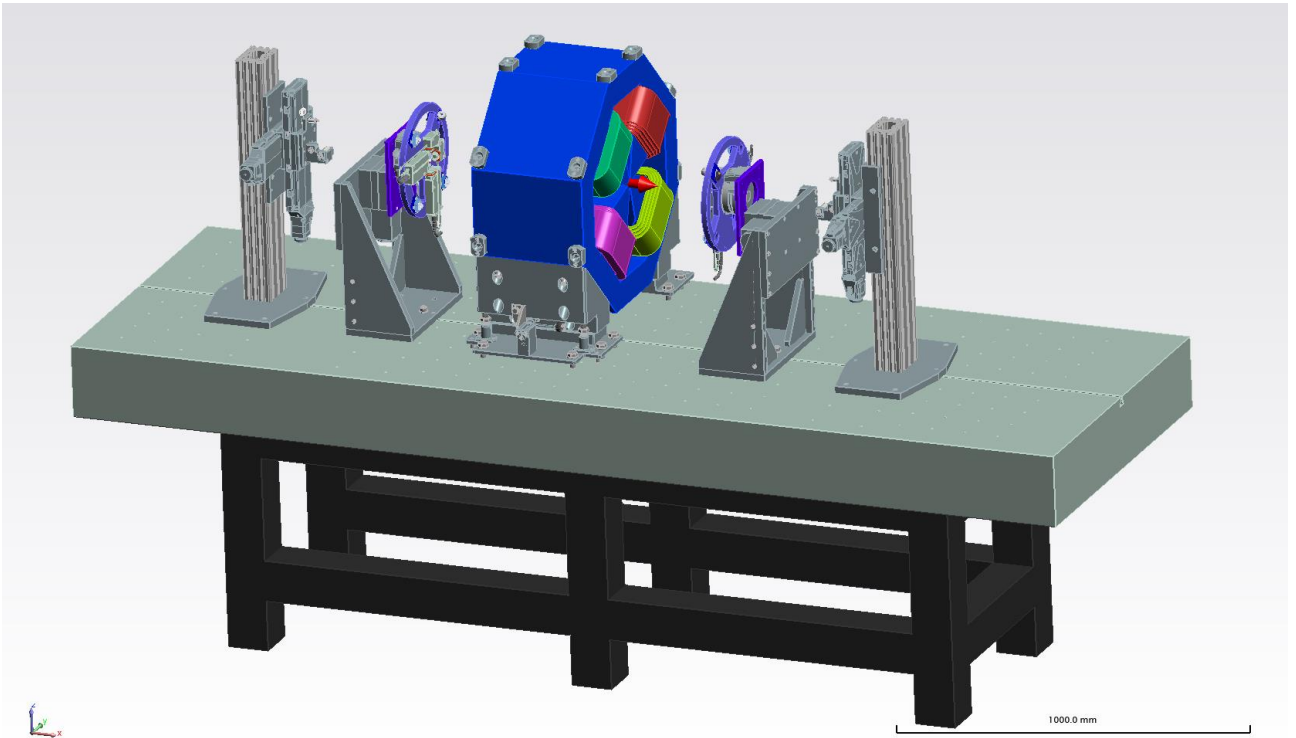


Figure 2: Resistive Magnet Measuring Bench [Daniel Thoden]

without allowing them to change the process or deviate from the routine.

After finishing the fiducialization, the system should show the quality of the result to the operator and indicate if a repetition is necessary. The alignment project engineer will be notified of the results, and, if everything is correct, the data should be automatically uploaded to the alignment database [2]. The alignment expert will be, of course, able to intervene in the process.

Principle

Measurements taken from the KOMs lie in the 2D Keyence coordinate system (KCS). The AIP has a rotating coordinate system (ACS) defined relative to the reference marks that are stationary with respect to the rotating AIP. The ACS is centered at the AIP's axis of rotation during the calibration process.

The wire measurements taken by KOMs will form a circle of points in the KCS. The center of this circle coincides with the axis of rotation of the rotational stage determined by observing the rotating reference marks. The AIPs and their KOMs are static during the magnet axis measurements. But they will rotate during the magnet fiducialization phase.

Transformation between the Keyence coordinate and the local coordinate systems is:

$$\mathbb{W}_L = \mathbb{R}_\omega \cdot (\mathbb{W}_K - \mathbb{C}\mathbb{R}_K) \quad (1)$$

where:

$\mathbb{W}_K = \begin{pmatrix} X_{W_K} \\ Y_{W_K} \end{pmatrix}$ are the coordinates of the wire in KCS,

$\mathbb{C}\mathbb{R}_K = \begin{pmatrix} X_{C\mathbb{R}_K} \\ Y_{C\mathbb{R}_K} \end{pmatrix}$ are the coordinates of the Center of Rotation in the KCS,

$\mathbb{W}_A = \begin{pmatrix} X_{W_A} \\ Y_{W_A} \end{pmatrix}$ are coordinates of the wire position in the local coordinate system,

ω is a fixed (referenced) angle between the ACS and the KCS axis and determines the rotation matrix \mathbb{R}_ω . It is determined during the calibration.

The wire position is conveyed to the 3D space by determining the position of ACS through the measurements. The two points of wire will form a line which will be considered the magnetic axis of the magnet and will form the X axis of the magnet coordinate system. The Z axis will be determined as a vector in the KCS. The accuracy of the determination of the Z axis needs to be investigated prior selecting this solution. Y axis will be complementary to the X and Z axes to form a Cartesian coordinate system. A solution for determining the origin comes from tactile measurements of the magnet's poles.

Laser Tracker Approach

During the fiducialization process, the alignment interface plate, containing the KOMs and fiducials, will rotate. The position of the alignment interface plate is monitored by a specially designed, precisely rotating spherically mounted reflector (SMR), which is permanently mounted to the interface. It is free to rotate and weighted in such a way as to maintain its approximate ($\pm 5^\circ$) orientation relative to a laser tracker. This rotating fiducial is called the precision rotating

datum (PRD). There are also three stationary fiducials on the AIP that primarily inform the angle between KCS and ACS.

As mentioned before, the measurements of the wire position from the KOMs create a circle, where the circle's center coincides with the center of rotation. The center of rotation is measured by taking repeated measurements of the PRD while rotating the alignment interface. For each magnet to be referenced, a circle is best-fitted through the measured positions of the PRD and its center is considered the center of rotation of the rotational stage. The process then continues by following the calculations described in the Principle section. In order to improve the precision of the fit, the radius of the circle can also be determined during the calibration process. The roll of the magnet is conveyed as an angle in the KCS. These linear stages are also referenced to a common coordinate system.

The SMRs used for this are going to be ceramic given that magnetic materials are not suitable. The stationary fiducial are designed as a three-points-of-contact nest with a retaining ring over the SMR. There was an extensive design process with a lot of prototyping using 3D print. The final version is currently being manufactured from aluminium by our workshop (MEA4).

A spatial scan of the rotating AIP with a laser tracker is currently not a viable option due to the uncertain synchronization between the laser tracker and KOMs.

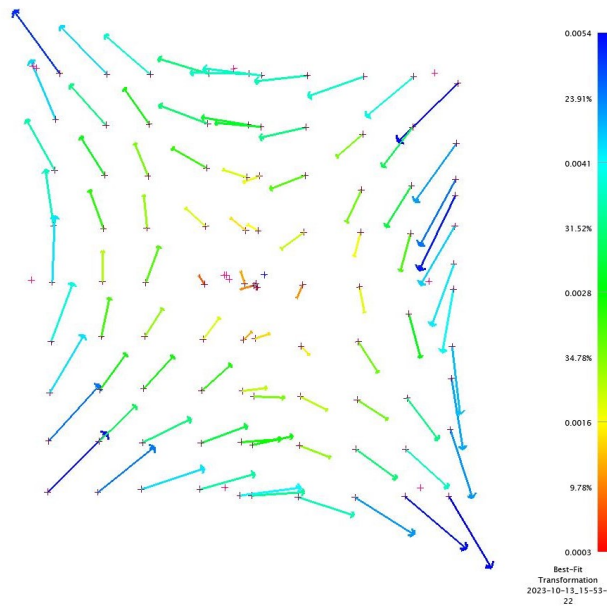


Figure 3: This shows the transformation between the KOM and CMM measurements. The saddle shape indicates the non-perpendicularity of the KOMs. The color scale indicates the size of the deformation in mm, along with percentiles of measurements the listed range.

Calibration The calibration process of the alignment interface uses a coordinate measurement machine (CMM). The KOM stand will be placed on the measurement surface of CMM in the same orientation as it will be later installed on the magnet measurement bench. This enables corrections or characterization of most of the imperfections of the system, including sag, tilt, and non-orthogonalities. The measurement of the fiducials can be performed by CMM tactile measurement of the reflective surfaces of the SMR. This will, in case of PRD, exclude the centering error of the corner cube placement within the sphere. If a gentle enough method for locking the SMR in place is found, the process could even correct for the imperfections in the PRD's mechanism. This option must be further assessed.

Through the calibration process, the KCS will be tied to the external fiducial markers on the alignment interface by determining the assembly-specific translation and rotation.

The mathematical correction for imperfections can be calculated and later applied. The orthogonalization of the non-perpendicular measurements from the KOMs is based on the an affine transformation with the iterative least square method. We are searching for the elements a, b, c and d of the affine transform matrix by minimizing difference between reduced CMM coordinates and transformed reduced KOM coordinates:

$$\begin{pmatrix} \bar{X}'_{K_i} \\ \bar{Y}'_{K_i} \end{pmatrix} = \begin{pmatrix} a & b \\ c & d \end{pmatrix} \cdot \begin{pmatrix} \bar{X}_{K_i} \\ \bar{Y}_{K_i} \end{pmatrix}, \quad (2)$$

where:

$\begin{pmatrix} \bar{X}'_{K_i} \\ \bar{Y}'_{K_i} \end{pmatrix}$ are rotated and orthogonalized reduced to centroid KOM coordinates,

$\begin{pmatrix} \bar{X}_{K_i} \\ \bar{Y}_{K_i} \end{pmatrix}$ are reduced to centroid measured KOM coordinates,

$\begin{pmatrix} a & b \\ c & d \end{pmatrix}$ is affine matrix the combined orthogonalization and rotation linear transformations.

The minimization will minimize the square difference between CMM measured reduced coordinates and KOM's reduced transformed coordinates. The rest is simple LSM.

During the referencing measurements of the KOMs and AIP, we ¹ have measured a grid of points where the KOMs observed the CMM probe, resulting in simultaneous and coincident CMM and KOMs measurements. After a best-fit transformation, the measurements displayed in Figure 3 clearly show the non-perpendicularity of the KOMs. I also learned during the PoC measurements that the Keyences measure better if they measure the shaft of the CMM's tactile probe and not the ruby ball at the end. We also found that changing the color of the shaft from reflective to black does not effect the KOMs reading.

Calibration would be tedious if done in the way the PoC was done: manually driving the CMM's probe and documenting the KOM and CMM coordinates in a labor intensive

¹ Measured with Matthew Laws and Florian Andresen

way. This is unacceptable beyond the PoC. Consequently, the design of the AIP was changed to add a special circular plate, to be inserted into the opening of the AIP during the calibration. This calibration insert will create a surface for the CMM probe to touch, so taking data from the KOMs and CMMs can be automated, which enables the use of a multitude of magnet measurement stands. We plan to have 4+1 measurement benches in the production phase, corresponding to 10 stands.

Simulations A simulation has been performed by Spatial Analyzer in order to determine the uncertainty in the calculated center of rotation (CoR) from laser tracker measurements. The laser tracker uncertainty employed is derived from experience with precise measurements of deformations (see “PETRA IV Girder Transport Tests” [3]). The results

Table 1: Uncertainty of Leica AT960 as per [3]

Quantity	Uncertainty
Horizontal angle	0.11 mgon
Zenith angle	0.42 mgon
Slope distance	4 μm + 1 ppm

using Table 1 shows, that 72 points around the circle must be measured to reach a center point accuracy of 1 μm . That represents a measurement every 5° of rotation. The relationship between the number of laser tracker measurements and the calculated center point uncertainty is tabulated in Table 2.

Table 2: Simulation results of CoR uncertainty vs number of points measured on the circle

Number of points	Uncertainty
9	4 μm
18	3 μm
36	2 μm
72	1 μm

Photogrammetry Approach

Photogrammetry is being explored² as an alternative for measuring the location of the alignment interface plates. The photogrammetry approach concept centers on automating the process by imaging the AIP only from a circular path above the measurement bench from a motorized rotating frame. We built a large frame spanning over the magnet and roughly 1.5 m above it. The rotating arm installed on the frame turns the camera in a 1.5 m radius. Tests and proofs of concepts are being done with a GSI Inc.’s photogrammetry system using the Nikon D700 camera, the 50 μm version, and V-STARs software. The setup can be seen on Figure 4.

² The photogrammetry work is being done in cooperation with Martin Noak.

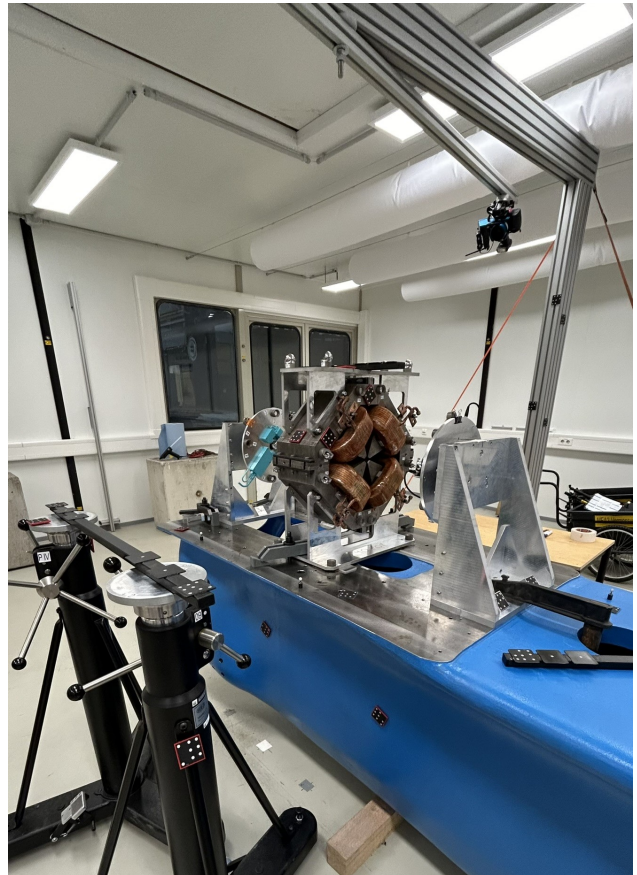


Figure 4: Photogrammetry setup with small KOM plates.

Relatively good results were achieved in initial feasibility tests, but optimization was needed to make the method applicable. Initially we used the same size of alignment interface plate as was used for the laser tracker approach, but larger the AIP plates were found to be more practical for this approach. The AIPs were enlarged by 150 mm to the design shown in Figure 5. This enhanced the visibility of the fiducials. The measurement area was then targeted with coded targets, scale bars, reflective ball targets, and spherical fiducial targets.

We measured³ with the photogrammetry setup in three different sets. First, we used small AIPs and experimented with the position of the fiducials, the setup, and the camera position. The fiducials were on the sides of the AIPs facing the magnet, which lead to decreased visibility. We measured a cluster of points with small differences in the radius. Here, the camera was now mounted on the frame and rotating above the setup. We also marked the angle of the rotation, because the V-STARs software has a problem with naming points if the position of points are too similar to the previously measured fiducial due to rotation.

Then for the next two sets, we used larger plates and measured four fiducials in a diamond shape cluster, with each fiducial at a slightly different radius. We used fiducials on the side of the AIP facing away from the magnet. One set

³ Measured with Martin Noak and Sebastian Albrecht.

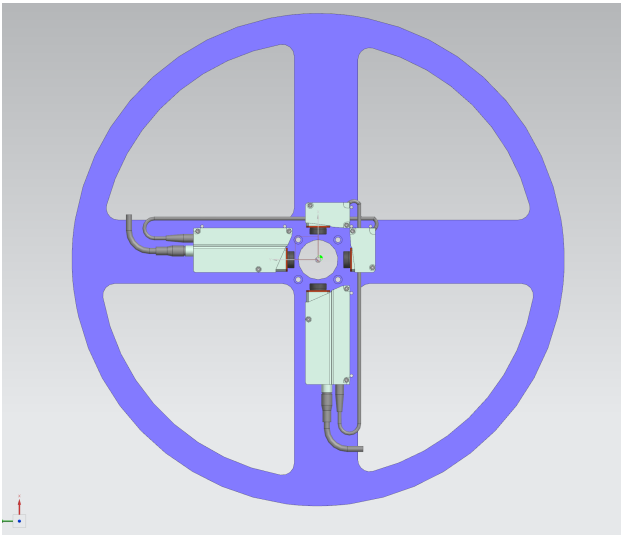


Figure 5: Large AIP for photogrammetry [Daniel Thoden]

had the camera hand-held, while the other had the camera on the rotating frame. The hand-held camera setup got slightly better results. The movements of the camera would be very difficult to mimic with an automated process.

Table 3 shows the maximum uncertainties of the measured points during the rotation of the AIP and the stationary magnets fiducials. The magnets fiducial uncertainties are significantly better, as expected, since they have a better geometry and more measurements than the points on the AIP. More images were taken with the small AIP, resulting in lower uncertainties.

Table 4 details the median differences between determinations of the centers of rotation (CoRs). In each phase, a rotating AIP was measured four times with the laser tracker, and four times by photogrammetry. These are independent measurements of the same rotating AIP, each circle using a different fiducial. "LT and Photogrammetry" shows the median of the differences between the two sets of four measurements, and reveals the systematic differences between the measurement methods.

Table 3: Photogrammetry results

Description	Max σ_{XYZ} AIP	Max σ_{XYZ} Magnet Fiducial
Small AIP, frame cam	23 μm	10 μm
Large AIP, hand cam	41 μm	20 μm
Large AIP, frame cam	58 μm	16 μm

All the results are at the level of the camera's accuracy or better. The next course of action is to borrow a camera with higher accuracy rating. The accuracy might be further improved by: using the whole reflective 1.5" targets in fiducial nests, and coded targets that can be referenced with tactile measurements. Another possibility to try is a setup with two cameras at different heights.

Table 4: Medians of differences in 2D magnitude of measured CoRs during large AIP measurements

Pass 1 - camera in hand	
CoR Data Source	Median of differences
Laser tracker	4 μm
Photogrammetry	6 μm
LT and Photogrammetry	21 μm
Pass 2 - camera on frame	
CoR Data Source	Median of differences
Laser tracker	3 μm
Photogrammetry	47 μm
LT and Photogrammetry	26 μm

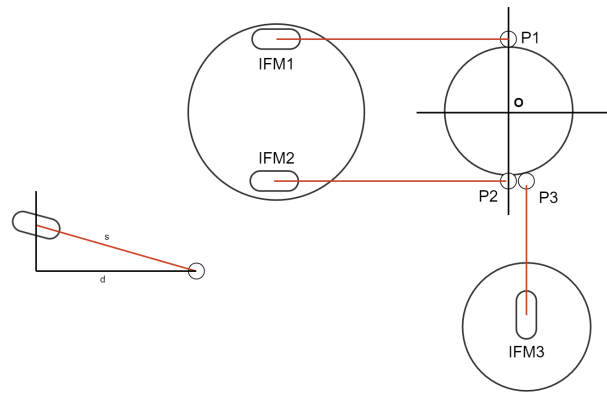


Figure 6: IFM Setup Scheme

INSTRUMENT PILLAR DESIGN

The previous pillar design was used in HERA, and has been tested both as an instrument stand for a laser tracker and as the reference network pillar.

Instrument pillars will be permanently attached to the floor in the measurement area. This creates forced instrument locations. These pillars will be necessary in the girder assembly area of the Girder Assembly Building (GAB) and in both climate-controlled rooms. One climate-controlled chamber, also in the GAB, serves as the final alignment measurement room. The other is in Halle 2, where the precise magnet referencing will take place. In total, there will be around 50 of those pillar.

Testing of the Pillar

Pillar testing informs the design of new instrument stands that are sufficiently stable despite vibration introduced by the supported instrument.

Deformations are introduced by a Leica AT960 laser tracker placed on top of the pillar as it maneuvers to measure the surrounding network of points. Scheme of the pillar measurements is in Figure 6. Three PicoScale interferometers (C03 heads) measure the transverse displacement and axial torsion of the instrument stand under test. They ob-

serve SMRs (0.5'') mounted to the pillar just under the laser tracker's mandrel by small magnets glued onto the structure. Measurements are performed in the environmentally stabilized room.

The unavoidable misalignments of the system are corrected geometrically. The corrections are calculated based on following equations: First, measured slope distances are reduced to horizontal plane using zenith angle Z :

$$d_i = s_i \cdot \sin Z_i, \quad (3)$$

horizontal distances are then reduced to displacements from initial positions and further processed to represent changes in 2D Cartesian coordinate system:

$$\Delta x = \frac{\Delta d_1 \cdot \sin(\delta) - \Delta d_2 \cdot \sin(\omega)}{2}, \quad (4)$$

where δ is the angle between the line between P_1 and O and the IFM_1 ,

ω is the angle between line P_1 and O and IFM_2 .

$$\Theta = \frac{\Delta x_1 - \Delta x_2}{D}, \quad (5)$$

where: D is the diameter of circle through P_1, P_2 and P_3 theoretically identical to $2 \times |P_1 O|$,

Θ is the angle of the axial torsion.

$$\Delta y = \delta d_3 \cdot \sin(\psi - \omega) - \frac{D}{2} (1 - \cos \Theta), \quad (6)$$

where: ψ is the angle between IFM_2 and IFM_3 .

HERA Pillar as an Instrument Pillar These pillars were meant as removable theodolite stands in the HERA tunnel. There was not enough space and the transport of material to the tunnel collided with the requirement of a forced instrument centering. Their stiffness and stability were not designed to withstand the forces applied by a modern laser tracker. The torque and inertia of a laser tracker are much higher than the gently hand-rotated theodolites previously used. Also the requirements for stability have changed to be under $1 \mu\text{m}$. Measurement setup can be seen in Figure 7. During the measurements⁴ of the dynamic deformations of the HERA pillar, immediately after the laser tracker being turned on, we observed very noticeable medium pitched audible vibrations. By a rough measurement it was determined that the frequency is $400 \pm 25 \text{ Hz}$. The dynamic deformations were in higher units of microns with peak to valley of $10 \mu\text{m}$ and $5 \mu\text{m}$. After these findings, it was obvious that this pillar cannot be used for the AT960 laser tracker, unless significant changes are made.

Concrete Block Pre-prototype Testing Instead of improving the design of the HERA pillar, we have decided, with the project mechanical engineers, to try a solution at the opposite extreme of the light and compact pillar: a bulky, multi-ton concrete block.

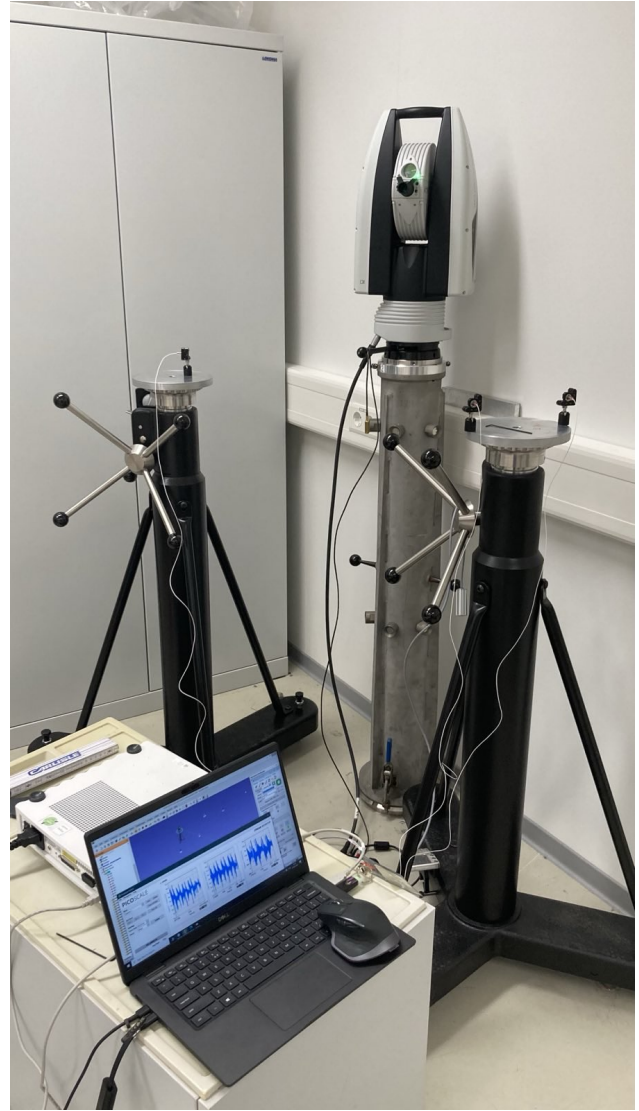


Figure 7: Testing of a HERA pillar as an instrument stand

More instrumentation was used for measuring⁵ the characteristics of the concrete pillar: two seismometers, 8 accelerometers, the laser tracker, interferometers, and a measurement arm. The measurement setup is shown in Figure 8. One seismometer (black cylinder with handle) was placed on top of the concrete pillar and one on the floor next to it. Measurement from these showed that at frequencies below 100 Hz, the pillar only slightly amplifies the frequency peaks coming from the ground. These are typical of DESY ground vibrations.

Three accelerometers were placed on the aluminium neck between concrete pillar and the laser tracker's mandrel, and three more were on the floor. As in the case of the seismometers, the results are the same in the low frequency region. Followed by a quiet region of 100 Hz to 150 Hz for both the floor and the neck. Floor continues to be quiet apart from

⁴ Measured with Sebastian Albrecht

⁵ Measured together with Norbert Meyners, Yvonne Imbschweiler, Ede Zabel and Tom Dobberstein.



Figure 8: Testing of the concrete block pillar preprototype

a small sharp peak at 200 Hz. However the laser tracker excites slowly rising peaks at 195 Hz, 270 Hz and 450 Hz. The measurements using interferometers were processed and in the low frequency region also agrees with the seismometers and accelerometers. There was a drift in one of the interferometers, despite it being warmed up, that could not be successfully filtered out. Therefore, the results from the interferometers will not be used.

The results clearly show path forward for future design of the prototype pillar: its first eigenfrequency should avoid the disturbance spectral peaks and be at least 100 Hz to 150 Hz.

A model for the instrument stand is being designed by a fine element analysis based on these prerequisites, with the intent to make it out of cast iron.

TOOL DEVELOPMENT

During the TDR phase various software tools were developed. Some for data processing, some as parts of the foreseen automated workflow. Following is the overview with short descriptions.

SAOpener to find and open SA, regardless of the executable's location on disk or version. and also checks the presence of the hardware lock. This is a preparation for the automation of the referencing process [4].

SA to Precise Planner converter [5] converts an SA's Instrument Composite Report into the input format of Precise Planner software [6]. This tool is is easy to adapt to any desired text output format.

Pillar Stability Calculation Tools is a set of scripts which processes the data measured by interferometers and laser tracker during the pillar stability test [7]. These are still being developed.

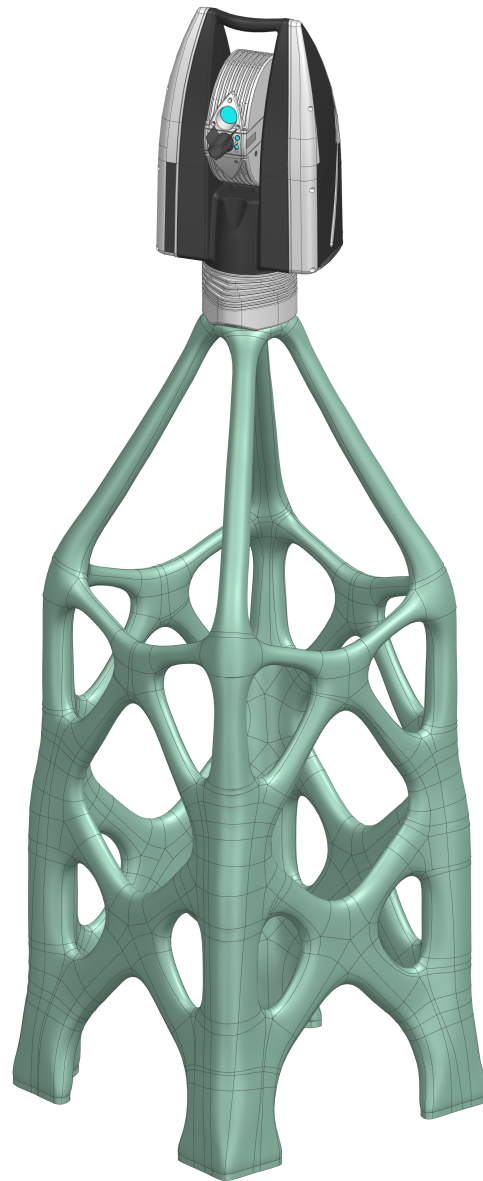


Figure 9: Intermediate topology optimization result for a support structure made of cast iron (EN-GJS-600), achieving a first eigenfrequency at 234 Hz [Normann Koldrack]

SUMMARY

The alignment of PETRA IV provides plenty of challenges. The accuracies of the alignment in the tunnel range from 30 μm to 100 μm at $P = 68\%$ depending on the element. Two crucial parts of the alignment, apart from final alignment, will be referencing the resistive magnets and the stability of instrumentation during referencing and final alignment of the magnet. This paper discusses key advancements in the search for ideal magnet referencing technique and in the design of the instrument pillars.

The referencing uncertainty is desired to be as low as 15 μm , including the magnetic axis search errors with the stretch wire, the stretch wire position measurements, and the referencing itself. Therefore new methods are being developed. The development includes a variety of experimental setups and proofs of concept, some of which are detailed in this paper.

The laser tracker approach is currently at the beginning of its prototyping phase. Stationary alignment interface plate fiducials await manufacturing and testing. We expect no issues with their precision. The precision rotating datum is being prepared for first prototype manufacturing. I introduced the principle and challenges of the novel laser tracker approach.

In the photogrammetry approach, we experimented with different geometries of the camera, the AIPs, and the fiducials. In all cases, we quickly got to the accuracy limits of the camera. The experiment validated the photogrammetry proof of concept as definitely a valid option. In the future, we have to prove that it can reach and exceed the required accuracy for referencing. Geometry plays a large role in the accuracy, and we need to take that into account when preparing the next test.

The parallel advancement in both approaches to referencing is necessary for risk mitigation, with photogrammetry approach hedging the highly experimental laser tracker approach. Development of these techniques will continue in parallel until one of them is fully validated and fulfills all the requirements with confidence.

There is a clear need for stable non-vibrating instrument stands in permanent positions. The previously used HERA pillars are inadequate, obviated by salient audible vibrations from their interactions with the laser tracker.

The initial requirements for design of a custom build instrument pillar shall be determined before the process starts. We determined the baseline specifications for the design of the new instrument pillar, though the use of abundant, albeit

sometimes misbehaving, instrumentation. In particular, that their first eigenfrequency should be at least 100 Hz and avoid the driving frequencies from the laser tracker.

ACKNOWLEDGEMENTS

Special thanks to Markus Schlösser (MEA2) who always brainstorms with me and helped me review the technical aspects of this paper.

I could not do without the help of Sebastian Albrecht, Martin Noak, Johannes Prenting, Yvonne Imbschweiler, and Petra Radomi (MEA2 - Department of Applied Geodesy); Daniel Thoden, Normann Koldrack, Norbert Meyners, and Matthew Laws (MEA1); Philipp Altmann and his group (MEA4); Uwe Eggerts and his group (MEA5); and Florian Andresen (ZMQS).

And the person responsible for the language corrections is, as always, Anthony Barker (MSK). Thank you.

REFERENCES

- [1] C. G. Schroer and DESY, *PETRA IV: upgrade of PETRA III to the Ultimate 3D X-ray microscope. Conceptual Design Report*, R. Roehlsberger, E. Weckert, R. Wanzenberg, I. Agapov, R. Brinkmann, and W. Leemans, Eds. Deutsches Elektronen-Synchrotron DESY, 2019, 259 pages : illustrations, diagrams. doi : 10.3204/PUBDB-2019-03613
- [2] M. Schlösser, "Coordinate Database at DESY," 14th International Workshops on Accelerator Alignment, Grenoble (France), 3 Oct 2016 - 7 Oct 2016, 3, 2016, p. 3. doi : 10.3204/PUBDB-2016-06681
- [3] J. Barker and M. Schlösser, "PETRA IV Girders Transport Tests," 16th International Workshops on Accelerator Alignment, Ferney-Voltaire (France), 31 Oct 2022 - 4 Nov 2022, 1, 2022, p. 6. <https://indico.cern.ch/event/1136611/contributions/5027108/>
- [4] Jana Barker, *SAopener*, version 1.0, 20, 2024. <https://github.com/Jadracka/GeodesyLibrary/blob/master/Helpers/SAopener.py>
- [5] Jana Barker, *SA to Precise Planner converter*, version 1.0, 20, 2024. <https://github.com/Jadracka/GeodesyLibrary/blob/master/PPInteraction/SA2PP.py>
- [6] M. Štroner, "Development of software for planning accuracy of geodetical surveying PreciSPlanner 3D," *Stavební Obzor [Civil Engineering Journal]*, vol. 19, no. 3, pp. 92–97, 2010.
- [7] Jana Barker, *Pillar Stability Calculation Tools*, version 0.9, 26, 2024. <https://github.com/Jadracka/PillarStabilityCalcs>